Finger Flexion Imagery: EEG Classification Through Physiologically-Inspired Feature Extraction and Hierarchical Voting

Daniel Furman*, Roi Reichart, Hillel Pratt
Technion – Israel Institute of Technology
Haifa, Israel
*dfurman@tx.technion.ac.il

***Abstract*—Accurate electroencephalography (EEG) classification of finger flexion imagery would endow non-invasive brain-machine interfaces (BMIs) with a much richer control repertoire. Traditionally, it has been assumed that non-invasive methods lack the resolution required for success on such a fine discrimination task. In this study, we challenged this assumption. EEG was acquired while subjects imagined performing individual and bimanual finger flexions. A new method of spatiotemporal and spectral feature extraction was applied, and multi-class support vector machine (SVM) classifiers were trained. Predictions and probabilities then served as inputs to a novel voting scheme, which output the system decision. The present approach achieved a mean population (n=15) accuracy of 30.86±1.76%, nearly twice the chance guessing level (16.71±1.68%) for the six-class task evaluated. Finger imagery is thus shown to be classifiable through EEG analysis alone.**

Keywords-EEG; BMI; Motor imagery; Spatiotemporal features; Spectral features; Multi-class SVM; Decision system

I. INTRODUCTION

Attempts have long been made to characterize the EEG encoding of voluntary finger movement [1], and more recently, to accurately decode and classify the activity patterns [2], [3]. Decoders have steadily progressed from sensitivity to single finger movement onset without any specificity [4], to left versus right hand discrimination [5], to distinguishing between movements by four fingers on the same hand [2] and pairs of fingers on the same hand [3] with above-chance accuracy.

Markedly, the research literature in this area is populated exclusively by reports on brain activity associated with actual, physical finger movements, in contrast to the BMI aim of decoding brain activity associated with imagined movements [6]. Most imagery research has instead focused on the somatotopically expansive and distinct right hand, left hand, legs and tongue [7], presumably, due to the assumption that the poor spatial resolution of EEG limits its ability to discriminate between signals emitted by the dense, overlapping neural ensembles responsible for finger flexion [8], [9]. If the challenge of accurately classifying individual finger flexion imagery could be met however, BMIs would be endowed with a substantially richer control command repertoire. In recognition of this potential, the current study sought progress in this direction.

II. METHODS

A. Subjects

Fifteen (15) right-handed (assessed by the Edinburgh Handedness Inventory), female and male volunteers, 18-30 years old, with normal hearing and motor function, and without a history of neurological or psychiatric disease, participated in the experiment. Subjects were paid for participating, and all procedures were approved by the institutional review board for experiments involving human subjects (Helsinki Committee).

B. Data acquisition

A 64-channel EEG cap (Electro-Cap International) with electrodes embedded according to the 10/20 and intermediate electrode locations 10/10 system was positioned on the subject's head. Each electrode well was filled with conducting gel (Electro-Cap International). A 9-mm disc electrode placed on the middle of the chin served as reference, and an electrode clipped on the left earlobe served as ground. Three electrodes recorded eye movements (EOG); two placed bilaterally near the outer canthus of each eye, and one below the right eye. To record electromyographic (EMG) activity, bipolar surface electrodes (Electro-Cap International) were positioned atop the thenar and hypothenar muscles of each hand, and filled with conducting gel. The cap-mounted and bipolar electrodes were connected to an EEG recording system (MicroMed). Potentials from all channels were amplified at 0.15-134.4 Hz, digitized with a 16-bit A/D converter, and sampled at 512 Hz. The impedance of each electrode was brought below 5 kOhm before the experiment began, and maintained at that level for the experiment's duration.

C. Setup

Subjects sat upright in an electrically shielded and acoustically isolated room, wearing headphones, with fingers on a response device resting in their lap. The custom-built device contained four buttons, for the thumb and fifth finger of each hand. Subjects were instructed to keep their eyes open and to avoid making any movements.

D. Paradigm

1) Stimuli: The experiment consisted of blocks in which auditory stimuli, delivered in a pseudo-random order with pseudo-random timing, cued subjects to imagine pressing certain buttons. Each stimulus had a 50 ms, linear volume rise time, 400 ms sustained volume, and 50 ms fall time, providing for easy perception. Pure tones (250 Hz and 1000 Hz) were used, whereby the lower tone cued imagined flexion of the thumb, and the higher tone cued imagined flexion of the fifth finger. Stimuli were delivered either to the left ear, right ear, or to both ears simultaneously. The lateralization of each stimulus cued the hand for imagining the flexion, with binaural tones cuing bimanual flexion imagery. A complex sound, delivered binaurally, cued the release of each flexion.

2) Timing: The duration of time separating 'press' and 'release' cues was pseudo-randomly set to either 1000, 1500, or 2500 ms, such that the experiment contained equal instances of press imagery of each duration. A rest period randomized between 1500-3000 ms intervened between press-release cycles (Figure 1). All stimuli were delivered using Presentation software (Neurobehavioral Systems) and recorded at a sampling rate of 40 kHz.

3) Practice: Subjects practiced finger flexion imagery while maintaining relaxed muscles (i.e. silent EMG) by viewing their EMG data in real-time as they imagined pressing and releasing response buttons, individually and bimanually. After a subject proved adept at maintaining silent EMG during motor imagery performance, the main portion of the experiment began

4) Blocks: The experiment proceeded through alternating blocks of cued imagined single-finger flexions, and cued imagined bimanual flexions. Single-finger blocks contained 120 cues in total (30 for each finger) while bimanual blocks contained 60 cues (30 for each bimanual pair). Blocks lasted 5-10 minutes. Dependent upon the subject's self-reported level of fatigue, the experiment contained 3-5 iterations, yielding a balanced data set of, on average, more than 100 events from each of the six finger imagery classes (4 single finger, 2 bimanual) per subject.

III. Data Preprocessing

Preprocessing was performed to ensure that brain activity alone was the input for feature extraction and classification. An available toolbox [10] was used to implement the cleaning procedure, which began with segmentation of the continuous EEG into epochs (-1000 ms to +2000 ms relative to cue), removal of DC bias, and second-order infinite impulse response (IIR) Butterworth filtering (0.1–24 Hz, 6 dB/octave slopes). Automatic voltage (±75 uV) and spectral thresholding (0-2 Hz at ±50 dB, 20-40 Hz at ±100-±25 dB) was employed to guide further visual inspection, and manual removal of trials irreparably affected by movement artifacts or miscellaneous electrical noise. Independent Component Analysis (ICA) [11] was applied to isolate artifact-contaminated components. Evaluation of the components was aided by the ADJUST algorithm [12]. Components reflecting non-brain activity were removed. Cleaned data from the 61 scalp electrodes were extracted, and segmented into 0-1000 ms (relative to cue) epochs.

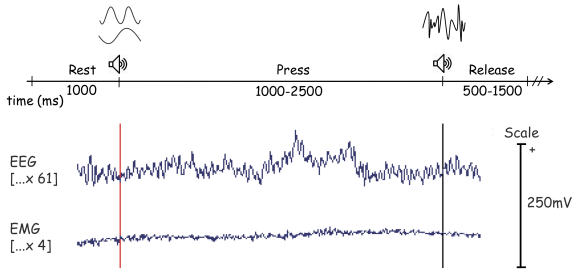

Figure 1. **Experimental time course.** Sample raw EEG and EMG from single channels aligned below a schematic outlining trial progression.

IV. Feature Extraction

A novel feature extraction method, inspired by domain-specific knowledge of the physiological encoding of imagined finger flexion, was applied. The following sections describe the new "Spiral Covawave" method, which is comprised of a multiple step process by which EEG data is rearranged, covariance matrices in time and space are computed, a wavelet decomposition is performed, data is reconstructed through a discrete filter bank, and outputs from each step are normalized to enable effective processing of the entire feature set within a uniform classification framework.

A. Spiral montage

Maximal smoothness across the sample space was a guiding objective. As channel-wise correlations are highest at nearest neighbor positions, the arbitrary ordering of data as acquired by the EEG system did not meet the smoothness objective, and so a new electrode arrangement was devised according to a heuristically approximated, shortest-path Hamiltonian solution.

The approximation began by defining the start position at one of the mastoid electrodes, being one of the two most remote relative to the remainder of the montage's spatial clusters. Next, a systematic spiral around the caudal-most section of the transverse plane was defined. Once every electrode in this first level had been passed, the spiral was elevated step-wise to the nearest electrode of the next level closer to the vertex. The result was a spiral montage that greatly improved data smoothness (Figure 2). Prior to feature extraction, data from all epochs were rearranged according to the spiral montage.

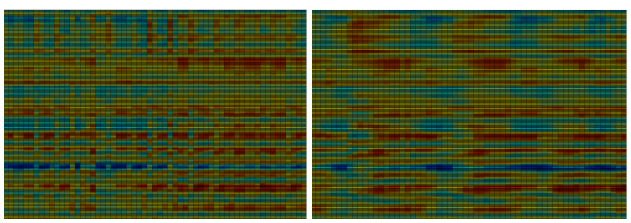

Figure 2. **Spiral montage rearrangement**. X-axis: channels, Y-axis: samples. Example data from a single epoch, as acquired through the default montage (left) and after rearrangement (right).

This work was supported by the Rappaport Family Institute for Research in the Medical Sciences.

B. Covariance features

Both the temporal covariance matrix and the spatial covariance matrix were computed through the empirical estimator

$$Cov = \frac{X^T X}{N-1}, \quad (1)$$

where $X = X_{ti}$ when computing covariance in time, where $X_{ti} \in R^{N \times C}$, and $X = X_{sp}$ when computing covariance in space, where $X_{sp} \in R^{C \times N}$. X corresponds to a single trial of data, where N is samples and C is channels.

C. Wavelet filter bank features

The wavelet transform, a convolution of the signal, $x(t)$, with an elementary function, $\psi_{s,\tau}(t)$, was performed. Formally defined as the following inner product:

$$W_\psi X(s,\tau) = \langle x(t) \mid \psi_{s,\tau}(t) \rangle, \quad (2)$$

where $\psi_{s,\tau}(t)$ are scaled and translated versions of the *mother wavelet* function $\psi(t)$, where

$$\psi_{(s,\tau)} = \frac{1}{|\sqrt{s}|} \psi\left(\frac{t-\tau}{s}\right), \quad (3)$$

such that s and τ respectively represent the scaling and translation parameters [13]. Scales and translations where defined discretely as the set

$$\{s = 2^{-j}, \tau = 2^{-j}k\} \text{ with parameters } j,k \in \mathbb{Z}. \quad (4)$$

A multilevel, one-dimensional wavelet decomposition was computed with j initialized to 7, and the wavelet function (ψ) defined as a biorthogonal wavelet with filters of 5. The transform was implemented in Matlab (The Mathworks), using Mallat's fast decomposition and reconstruction algorithm [14]. Data was then reconstructed through eight discrete frequency banks (7 details and the approximation).

D. Normalization

Each category of extracted features was normalized independently according to a common procedure, beginning with calculation of the feature's z-score through

$$z_{ft} = (Y - \mu)/\sigma, \quad (5)$$

where Y is the unrolled feature, μ is the feature's population mean, and σ the feature's standard deviation. The normalized feature vector is then computed by

$$\hat{Y} = \frac{Z_{ft}}{\max|Z_{ft}|}. \quad (6)$$

After normalization, all feature vectors were concatenated, and labeled vectors were filed into a feature matrix per subject.

E. Windowing

The Spiral Covawave method was applied to 32 windows of data derived from each 1000ms epoch. The minimum window was 80 samples (154.3ms), the maximum 400 samples (779.3ms), with sliding distances of 40 samples (77.15ms).

V. Classification

A. Phase I. Learning and Cross-Validation

A one-versus-one multiclass Support Vector Machine (SVM) with a linear kernel was employed using an available software package [15]. As our dataset contained 6 classes, a total of 15 binary classifiers, each trained to distinguish between a pair of classes, were constructed. The Max-Wins decision rule determined the system's output, whereby each new example was classified by every binary classifier, and the class that received the highest number of votes was selected. In case of ties, assignment was made to the class with the lowest index.

For every subject, feature matrices were processed through a 10-fold cross-validation procedure. Validation folds were generated through random sampling, using time information to seed the random number generator. To train and test the primary-level SVMs, at each fold 80% of the data was used for training, 10% for tuning the hyperparameter C, and the remaining 10% were used as an unseen test set. Fold indices, once generated for cross-validation testing of features corresponding to the first window, were kept constant for the remaining thirty-one windows. Posterior probability estimates were also computed, by mapping distance-from-hyperplane values to prediction accuracies through the training of a secondary-level sigmoid function [16].

B. Phase II. Hierarchical Voting

A persistent challenge to BMI technology is adapting to inter-subject variability. One technique for doing so is the selection of personalized time windows for feature extraction that isolate the most discriminative information per subject. Here, personalized window selection was automated, with the three windows corresponding to the highest accuracies during hyperparameter tuning chosen as inputs for the voting scheme.

During testing, the three selected windows' classifiers output their predictions along with posterior probability estimates into a decision function that made the final classification according to the rule,

$$\mathrm{D} = \begin{cases} \wp, & if \quad 1A_V = 1B_V = \wp \\ \Diamond, & if \quad 1A_V = 1C_V = \Diamond \\ \ell, & if \quad 1B_V = 1C_V = \ell \\ \aleph, & if \quad 1A_V = 1B_V = 1C_V = \aleph \\ \xi & if \quad 1A_V \neq 1B_V \neq 1C_V \end{cases}, \quad (7)$$

where $1A_V, 1B_V, 1C_V$ are the predictions (i.e. votes) of the first level SVM classifiers for windows A, B, and C

respectively; and $\wp, \Diamond, |, \aleph$ are the labels predicted. Hence, if at least two classifiers agree, their prediction becomes the system's decision D. In the case that all first level classifiers disagree, the decision ζ signals the system to evaluate probability estimates from the secondary-level sigmoid function. Canvassing of the secondary level information is crude, with a strict winner-take-all rule presiding:

$$D = \begin{cases} \wp, & if \quad 2A_P > 2B_P \;\&\; 2C_P \quad and \quad 1A_V = \wp \\ \Diamond, & if \quad 2B_P > 2A_P \;\&\; 2C_P \quad and \quad 1B_V = \Diamond \\ |, & if \quad 2C_P > 2A_P \;\&\; 2B_P \quad and \quad 1C_V = | \end{cases} \tag{8}$$

where $2A_P, 2B_P, 2C_P$ are the second-order probabilities associated with the first-level predictions for window A, B, and C respectively; and $\wp, \Diamond, |$ are the labels predicted at the first level. The empirical guessing level was estimated by random permutation of labels during testing.

VI. Results

The mean population accuracy for the six-class task was 30.86 ± 1.76%; nearly double the guess level of 16.71 ± 1.68%. The best performance was for subject 2, at 36.2 ± 6.75%, the worst for subject 3, at 22.83 ± 4.13%. The voting scheme obtained the highest accuracy in comparison to any single window classifier for 9 of the 15 subjects, with a mean improvement of 1.44 ± 0.89% over the best single classifier.

VII. Discussion

This study aimed to use EEG data exclusively to classify imagined finger flexions. A 6-class task was designed that challenged a classifier to distinguish between imagery of individual as well as bimanual finger movements. High accuracy was obtained by deploying a novel feature extraction and voting scheme, achieving a population mean accuracy of 1.85 times chance levels, outperforming classifiers previously reported in the literature on EEG associated with actual movements, such as [2] (1.71 times chance) and [3] (1.52 times chance). It is worth noting that the classifier performed above chance for every subject (n=15), a non-trivial accomplishment given the challenge of the 6-class task. The classifier was also efficient: once trained, it classified new examples within tens of milliseconds. Furthermore, and significantly, the results reported here pertain to purely imagined finger movements decoded from EEG - the first such report in the literature to the best of the authors' knowledge.

While the hierarchical voting scheme did achieve higher accuracies across the population than any single classifier, it should be observed that its improvement over the best single window classifier was slight compared to the great leap in accuracies that would be expected if the three windows each contained discriminative, non-redundant information. It is therefore fair to regard the accuracies obtained here as approaching the apex of what is achievable given this feature set, which itself represents an extensive capture of physiological-relevant information. In the future, incorporating non-linear feature induction through deep learning, or adopting a graph-based approach that integrates similarity measures and clustering, may potentially boost classifier performance further.

VIII. Conclusion

The new Spiral Covawave method, which extracted the spatiotemporal and spectral features of brain activity associated with imagined finger flexion, was effective, and complemented by a hierarchical voting scheme that generated accurate predictions. Finger movement imagery, commonly assumed to be beyond EEG's resolution, is thus found to be decodable. With more attention from the non-invasive BMI community, finger imagery classification can be improved and applied to significantly expand the control command repertoire.

Acknowledgment

Thank you to Nadia Goldberg-Nahmany, Naomi Bleich and Nomi Mittleman for methodological support.

References

[1] L. Deecke, B. Grözinger, and H. H. Kornhuber, "Voluntary finger movement in man: cerebral potentials and theory," Biol. Cybern., vol. 23, no. 2, pp. 99–119, 1976.

[2] F. Quandt, C. Reichert, H. Hinrichs, H. J. Heinze, R. T. Knight, and J. W. Rieger, "Single trial discrimination of individual finger movements on one hand: a combined MEG and EEG study," Neuroimage, vol. 59, no. 4, pp. 3316–3324, 2012.

[3] K. Liao, R. Xiao, J. Gonzalez, and L. Ding, "Decoding individual finger movements from one hand using human EEG signals," PLoS One, vol. 9, no. 1, pp. 1–12, 2014.

[4] D. Lisogurski and G. E. Birch, "Identification of finger flexions from continuous EEG as a brain computer interface," in Proceedings of the 20th Annual International Conference of the IEEE Engineering in Medicine and Biology Society, vol. 20, Biomedical Engineering Towards the Year 2000 and Beyond, vol. 4, pp. 2004–2007, 1998.

[5] J. Lehtonen, P. Jylänki, L. Kauhanen, and M. Sams, "Online classification of single EEG trials during finger movements," IEEE Trans. Biomed. Eng., vol. 55, no. 2, pt. 1, pp. 713–20, 2008.

[6] J. Wolpaw and E. W. Wolpaw, Brain-Computer Interfaces: Principles and Practice. Oxford University Press, 2012.

[7] A. Vuckovic, "Non-invasive BCI: how far can we get with motor imagination?," Clin. Neurophysiol., vol. 120, no. 8, pp. 1422–1423, 2009.

[8] W. Penfield and E. Boldrey, "Somatic motor and sensory representation in the cortex of man as studied by electrical stimulation," Brain, vol. 60, pp. 389–443, 1937.

[9] M. H. Schieber, "Constraints on somatotopic organization in the primary motor cortex.," J. Neurophysiol., vol. 86, no. 5, pp. 2125–43, 2001.

[10] A. Delorme and S. Makeig, "EEGLAB: An open source toolbox for analysis of single-trial EEG dynamics including independent component analysis," J. Neurosci. Methods, vol. 134, no. 1, pp. 9–21, 2004.

[11] S. Makeig, A. J. Bell., T.-P. Jung, and T. J. Sejnowski, "Independent component analysis of electroencephalographic data," Adv. Neural Inf. Process. Syst., vol. 8, pp. 145–151, 1996.

[12] A. Mognon, J. Jovicich, L. Bruzzone, and M. Buiatti, "ADJUST: an automatic EEG artifact detector based on the joint use of spatial and temporal features," Psychophysiology, vol. 48, no. 2, pp. 229–240, 2011.

[13] S. Mallat, A Wavelet Tour of Signal Processing. Academic Press, 1998.

[14] S. Mallat, "A theory for multiresolution signal decomposition: the wavelet representation," Pattern Anal. Mach. Intell. IEEE Trans., vol. 11, no. 7, pp. 674–693, 1989.

[15] C. Chang and C. Lin, "LIBSVM : a library for support vector machines," ACM Trans. Intell. Syst. Technol., vol. 2, pp. 1–39, 2011.

[16] J. Platt, "Probabilistic outputs for support vector machines and comparison to regularized likelihood methods," Advances in Large Margin Classifiers, A. Smola, P. Bartlett, B. Scholkopf, and D. Schuurmans, eds., pp. 61–74. MIT Press, 2000.